Effect of Locally Loosened Soil on Wave Propagation

M. Otsubo
Institute of Industrial Science/The University of Tokyo, Tokyo, Japan, otsubo@iis.u-tokyo.ac.jp

Y. Nakata[1], U. Ali[2], R. Kuwano[3]
Institute of Industrial Science/The University of Tokyo, Tokyo, Japan, y-nakata@iis.u-tokyo.ac.jp [1], umairali@iis.u-tokyo.ac.jp [2], kuwano@iis.u-tokyo.ac.jp [3]

ABSTRACT: In-situ down-hole or cross-hole wave surveys are useful as a means of measuring spatial distribution of elastic wave velocities. However, detecting an existing subsurface cavity using this method is not easy, partially because the characteristics of wave propagation around a cavity are not fully understood. This contribution aims to develop a better understanding of how elastic wave signals are affected due to locally loosened soil around a subsurface cavity. Laboratory model tests are conducted, and it was found that compression waves propagating near to the cavity decelerate and attenuate, and frequency-domain responses are also affected by the local loosening. To understand particle-scale responses of loosened soil during elastic wave propagation, discrete element method simulations are adopted. Two types of soil elements composed of dense-loose mixed layers are examined; the simulation results reveal that the wave velocities are an averaged response of the entire soil element, whereas the frequency response is dominated by the loosest portion of the soil element. Besides, a reflection of wave energy is observed at a boundary where the soil density changes sharply.

Keywords: wave propagation; density; cavity; discrete element method; model test

1. Introduction

In-situ down-hole or cross-hole wave surveys (P- and S-wave velocity logs) are useful as a means of measuring spatial distribution of compression (P-) and shear (S-) wave velocities. Elastic wave velocities can be directly related to soil stiffnesses that are essential parameters for geotechnical engineering design, particularly for site response analyses (Atkinson [1]; Clayton [2]).

Recently, an increasing number of sinkhole problems in developed cities have been reported. A sinkhole occurs when a subsurface cavity grows and the pavement above the cavity cannot sustain the overburden loads. Thus, this failure can be prevented effectively if an efficient cavity detection method is established. The ground-penetrating radar method is widely used; however, the application is limited to cavities located at shallower ground (< 1.5 m). Consequently, engineers seek an alternative way to detect a subsurface cavity using conventional wave propagation surveys, e.g. surface wave surveys. However, Kominami [3] reported that surface wave surveys are not always effective to find cavities due to a lack of understanding of how waves propagate around a subsurface cavity.

Nakata [4] conducted laboratory model experiments where P-wave propagation through a model ground having a subsurface cavity was investigated using planar piezoelectric plates, referred to here as the disk transducers (DTs). Nakata found that P-waves decelerate and attenuate due to loosing of soil around a cavity, particularly for a large cavity. Frequency domain responses are also affected depending on the size of the cavity. Details of the measurement system and results are discussed below.

Ali [5] assessed soil loosening phenomena using the 3D discrete element method (DEM) where a suction-tension model was implemented to better consider partially saturated conditions. Nakata [4] adopted the DEM model proposed by Ali [5] and investigated how P-waves propagate around a cavity. As a relatively large inter-particle suction was adopted, soil loosening effects on P-wave signals were not fully understood.

The present study aims to understand how elastic wave signals are affected by locally loosened soil around a subsurface cavity. A series of DEM simulations are performed to assess particle-scale responses of loosened soil considering two types of soil elements composed of dense-loose mixed layers.

2. Laboratory experiments

As a part of this study Nakata [4] reported experimental results of P-wave propagation though a partially saturated ground having a subsurface cavity. This section gives a brief summary of the experimental method and the key findings.

2.1. Model test approach

A cylindrical model ground (300 mm diameter and 200 mm height) with a capacity of water supply through two bottom holes, was used (Fig. 1). Uniformly graded silica sand with a median particle size (D_{50}) of 0.5 mm was used. As a preliminary experimental case, an intermediate density, relative density (Dr) of 50%, was selected as a target density. Dr = 50% was achieved by controlling the drop-height in the air-pluviation method.

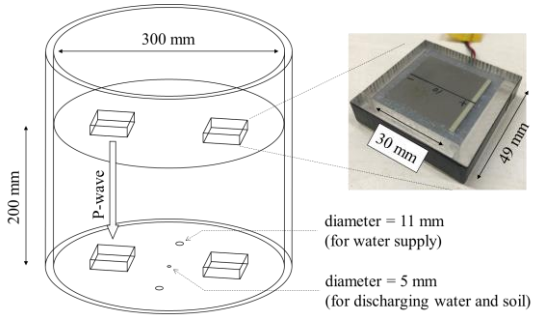

Figure 1. Test apparatus and piezoelectric plates (DT).

Two pairs of DTs were placed on the bottom and top of the ground (Fig. 1). A surcharge of 2.7 kPa was applied on the top surface uniformly to ensure good contacts between DTs and the ground surface.

The dry ground was saturated by raising the water level to the surface through the two holes at the base. The partially saturated ground was prepared by draining the water through the same holes; the partially saturated ground is termed as 'No cavity'. After the water level was raised to 100 mm from the bottom, soil and water were discharged simultaneously from the center hole at the base having 5 mm diameter (Fig. 1); this process left a small cavity, termed as 'Cavity S' (Fig. 2). After raising the water level to 150 mm from the bottom, soil and water were discharged to create a larger cavity, 'Cavity L'.

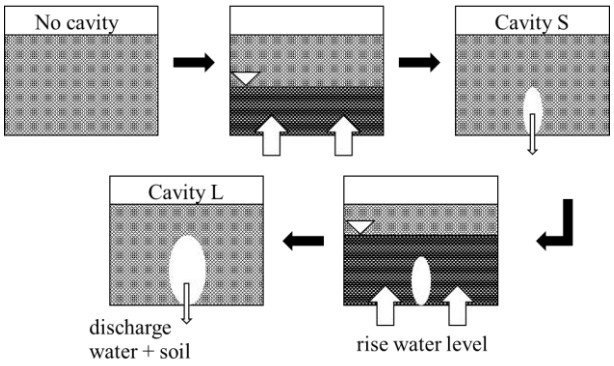

Figure 2. Procedure for creating a cavity in a model ground.

2.2. Model test results

A cross-section of the model ground 'Cavity L', is shown in Fig. 3. The shape of 'Cavity S' was deduced from the volume of discharged soil with a similar shape as 'Cavity L' (Fig. 3). Wave measurements were conducted along the vertical line connecting two DTs, located 20 mm away from the side of the cavity (Fig. 3). A single period of a sinusoidal pulse having input frequencies of 2~30 kHz was given from the transmitter DT to generate P-waves from the top surface.

The P-wave velocity (V_P) decreased as the size of the cavity increased, where the reduction of V_P compared with 'No cavity' case was 7.8% and 27.8% for 'Cavity S' and 'Cavity L' cases, respectively (Table 1). The maximum frequency that propagated through the model ground, i.e. lowpass frequency (f_{lp}), also decreased as the size of the cavity increased. The f_{lp} values for 'Cavity S' and 'Cavity L' cases were lower by 19.7% and 59%, respectively, from 'No cavity' case (Table 1). Thus, it is inferred that the growth of the cavity affects f_{lp} more sensitively compared to V_P.

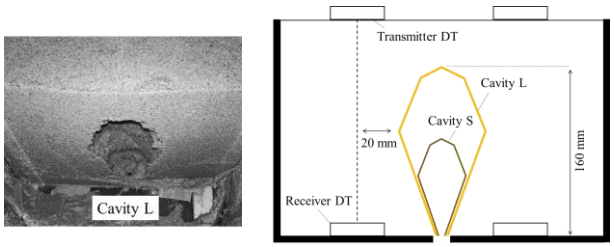

Figure 3. Cross-section of the model ground after the test.

Table 1. Experimental data for V_P and f_{lp}, reduced from 'No cavity'

	V_P : m/s		f_{lp} : kHz	
No cavity	205	-	18.8	-
Cavity S	189	-7.8%	15.1	-19.7%
Cavity L	150	-27.8%	7.7	-59.0%

3. Modelling approach

The decrease in both V_P and f_{lp} observed in the model test (Table 1) might be caused by locally loosened soil near to the cavity. Otsubo et al. [6] reported that both V_P and f_{lp} are lower for loosely packed granular materials. Following the DEM approach proposed by Ali [5], Fig. 4 illustrates the extent of loosened soil due to the formation of a cavity. Considering the wave path adopted in the model test (Fig. 3), a vertical column of the sample in the vicinity of the cavity can be ideally modelled as a binary-layered packing as schematically shown in Fig. 4 where the upper half contains denser packing and the lower half contains looser packing (*binary case*). However, the change in the density may not be always sharp; therefore, another packing having a varying density was also considered in this study (*varying case*). Several simplifications for these models were made as below.

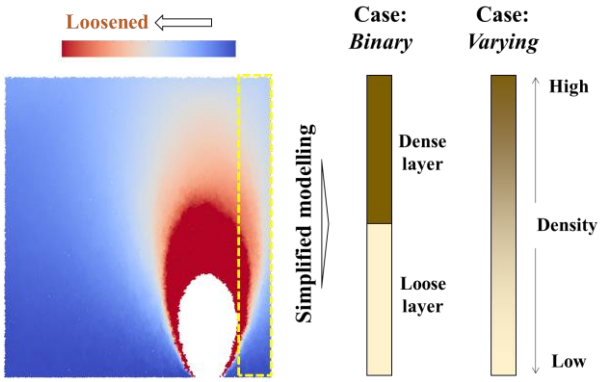

Figure 4. Schematic of the modelling approach.

4. Sample preparation and wave excitation

The DEM simulations were performed using granular LAMMPS software (Plimpton [7]). To simplify the complicated model test condition, mono-sized spherical particles (D = 2 mm) were used under dry conditions with typical material properties of glass beads (specific density of 2.5, Young's modulus of 71.6 GPa, Poison's ratio of 0.23); they were compressed with a servo control to reach an isotropic confining stress of 100 kPa using a mixed periodic and wall boundaries as illustrated in Fig. 5. The effects of gravity were not considered in this study.

Regarding the *binary case*, interparticle frictions (μ) of 0.01 and 0.5 were used for the upper and lower half of the sample, respectively, to control the density during the isotropic compression. When two particles with different μ values are in contact, an intermediate value of μ = 0.25 was used. For the *varying case*, μ values varying from 0.01 to 0.5 were used (from top to bottom) where the sample was divided into 50 layers with corresponding μ values depending on their vertical (Z-) positions. When particles having different μ values are in contact, an average value of μ was adopted for inter-particle responses.

A simplified Hertz-Mindlin contact model was adopted to calculate contact responses following the Itasca Consulting Group [8]. For the *binary case*, void ratio (e) values are 0.697 for the loose part and 0.565 for the dense part, with an overall e of 0.628. For the *varying case*, e changes gradually, and the mean e value is 0.662.

P- or S-waves were generated by translating a wall boundary in the Z- or X-direction, respectively. A sinusoidal pulse having a frequency of 20 kHz and a peak-to-peak amplitude of 5 nm was adopted.

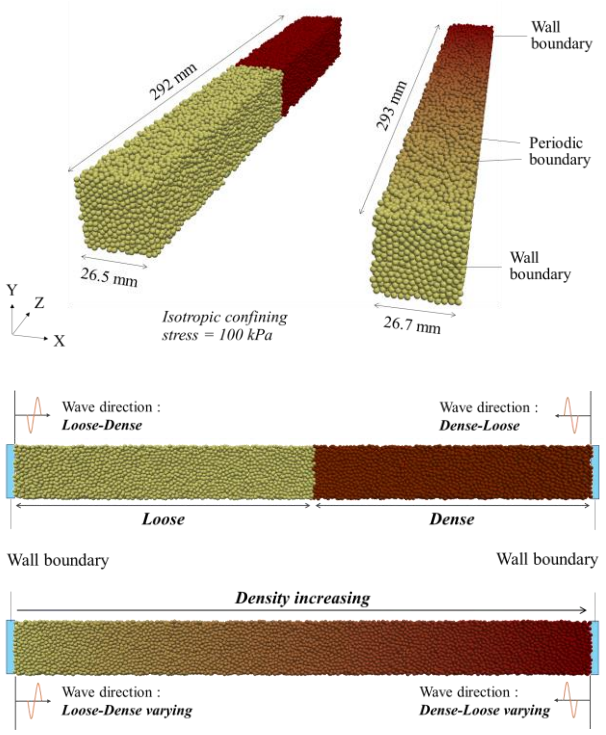

Figure 5. Tested DEM samples for wave propagation simulations. The color of particles corresponds to the value of friction coefficient (μ) where lighter color (larger μ) indicates looser packing.

5. Effects of a sharp change in density

5.1. Wave propagation velocity

The displacement of particles along a chain of the middle core of the sample was analyzed where particle displacements for Z- and X-direction are plotted for P- and S-waves, respectively. Besides, two directions of wave propagation are considered: excited from the loose packing (loose-dense), and vice versa (dense- loose).

Figure 6 shows the particle displacement during the P-wave propagation in a temporal and spatial space for the *binary case*. The darker color corresponds to a coherent wavefront that propagates linearly with time and distance. The slope in the distance-time relationship gives V_P. When the coherent wavefront enters the dense/loose layer, an increase/dcrease in V_P is observed. This is more clear when P-waves enter from the dense to loose layer. Regression analyses on the slopes give V_P = 343 m/s for the loose layer and V_P = 528 m/s for the dense layer.

Figure 7 shows the particle displacement during the S-wave propagation for the same sample (*binary case*). The slope of coherent wavefront in the distance-time space gives S-wave velocity: V_S = 212 m/s for the loose layer and V_S = 341 m/s for the dense layer, respectively. From Figs. 5 and 6, the wave velocity measured for the entire sample can be an averaged value for the overall packing.

For both P- and S-waves, a reflection of propagating waves at the boundary between the loose and dense layers is observed, irrespective of the direction of wave propagation. This reason is discussed further below.

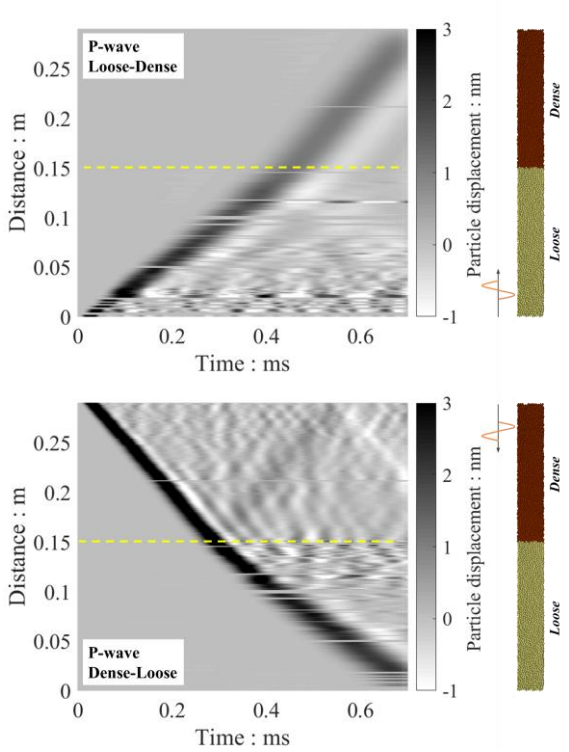

Figure 6. Time-distance plot for P-wave propagation along the binary sample (top) Loose to dense (bottom) Dense to loose.

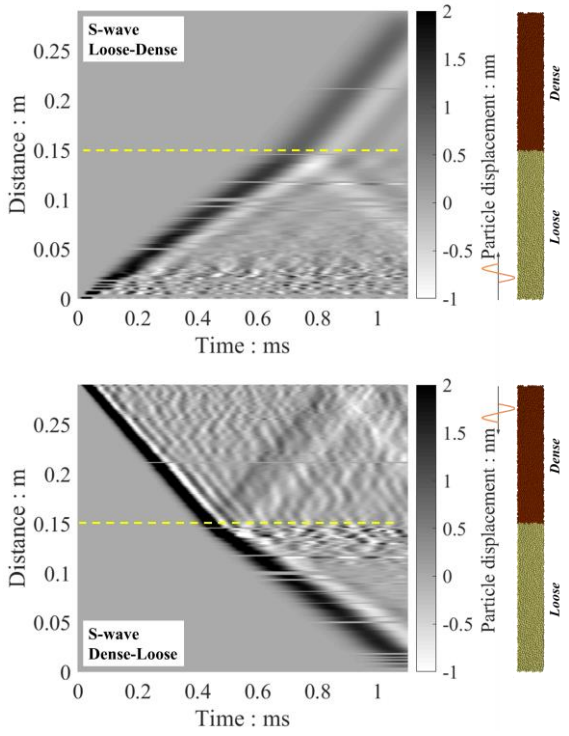

Figure 7. Time-distance plot for S-wave propagation along the binary sample (top) Loose to dense (bottom) Dense to loose.

5.2. Frequency filtering

A granular assembly acts as a lowpass filter against stress/sound waves propagating through the assembly (Lawney and Luding [9]; Mouraille and Luding [10]; Santamarina et al. [11]), and the lowpass frequency (f_{lp}) depends on the packing density, stress level (Otsubo et al. [6]) and the particle size (Dutta et al. [12]). To the authors' knowledge, however, the effects of sharp or gradual change in the packing density on the characteristics of frequency filtering have not been investigated.

Figure 8 shows spatial distribution of the frequency contents of P-waves where fast Fourier transform was applied to the displacement of each particle along the core of the sample. For the loose-dense condition (*binary case*), the high-frequency contents observed near to the wall is filtered sharply to reach a stable lowpass frequency (f_{lp}) of about 10 kHz, and no significant change is evident at the boundary of the two layers.

When P-waves are excited from the dense side, the f_{lp} value reaches about 25 kHz in the dense layer; however, it drops sharply to about 10 kHz when the waves enter the loose layer. Unlike the case for V_P, the residual f_{lp} value is determined by the lowest value of f_{lp} in the binary layer, i.e. the loose packing dominates the overall f_{lp}.

Figure 9 shows equivalent plots with Fig. 8 for S-waves. The overall reponses of the S-waves are similar to that of P-waves; however, the f_{lp} values observed for S-waves are slightly lower compared with that for P-waves. This is probably because the tangential contact (inter-particle) stiffness is lower than the normal contact stiffness for the Hertz-Mindlin contact model adopted in this study, and the S-wave mode is more influenced by the tangential contact stiffness.

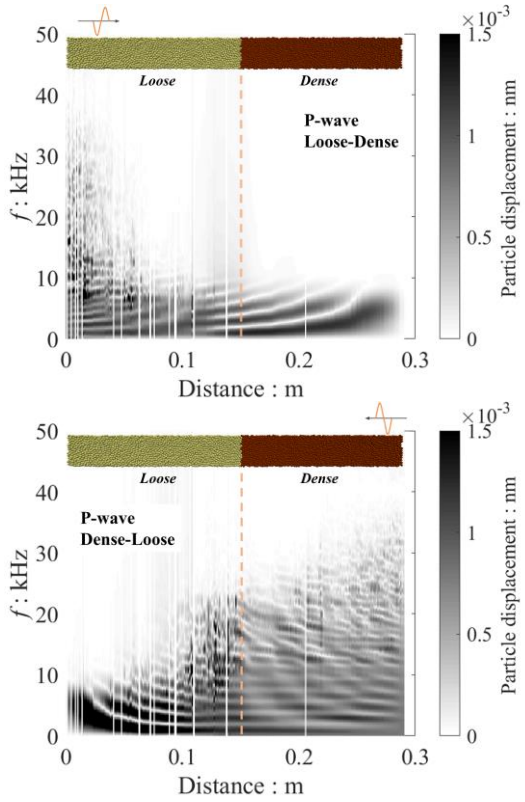

Figure 8. Frequency filtering for P-waves along the binary sample (top) Loose to dense (bottom) Dense to loose.

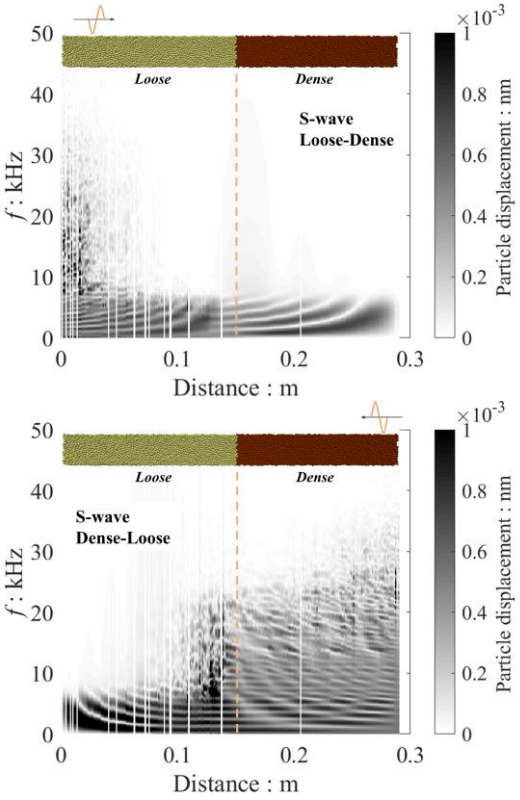

Figure 9. Frequency filtering for S-waves along the binary sample (top) Loose to dense (bottom) Dense to loose.

6. Responses of gradually loosened soil

As discussed above, the reflection of elastic waves is probably caused by a sharp change in the sample density, which is not always the case for the cavity problem considered here (Fig. 4). Referring to Fig 5, dynamic wave responses of a sample having varying density values (*varying case*), was examined. Since both P- and S-waves exhibit qualitatively similar results, the following discussion is based on S-wave data.

Figure 10 compares the particle displacement during the S-wave propagation along the sample with varying density. A gentle speed-up of the wavefront is evident when S-waves propagate from looser to denser side. In contrast, a gradual speed-down is observed when propagating from denser to looser side. For both cases, the reflection of waves is not obvious.

Figure 11 shows the spatial distribution of the frequency contents where the *loose-dense varying case* is almost identical to the equivalent plot in Fig. 9 (loose-dense). However, for the *dense-loose varying case*, gentle filtering of high-frequency contents is confirmed.

7. Theoretical interpretation of reflection

From the distance-time plots in Figs. 6 and 7, a reflection of propagating waves at the boundary between the dense and loose layers is observed, which can be related to the difference in the acoustic impedance (Z_I), defined as a product of bulk density (ρ) and V_P, i.e. $Z_I = \rho V_P$. The reflection coefficient of wave energy can be expressed as $R_I = (Z_I^d - Z_I^l)^2/(Z_I^d + Z_I^l)^2$ where the superscripts of d and l stand for dense and loose,

respectively. For the binary sample, R_I = 0.063; approx. 6.3% of wave energy can be reflected at the boundary.

The overall elastic wave velocity (V) can be found as $V = (V^d t^d + V^l t^l)/(t^d + t^l)$ where t is the time duration of wave propagation for the *binary case*. In contrast, the f_{lp} value is dominated by the lowest f_{lp} value in the wave path; this can be applied to both *binary* and *varying* cases.

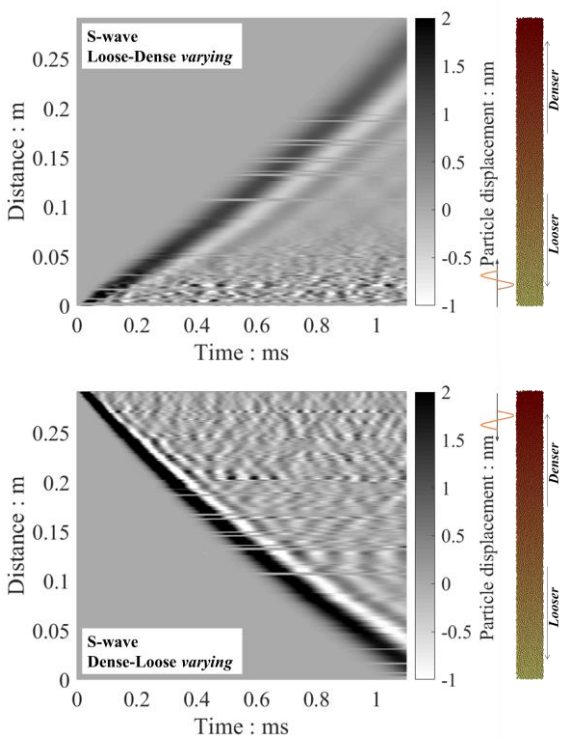

Figure 10. Time-distance plot for S-wave propagation along the varying sample (top) Loose to dense (bottom) Dense to loose.

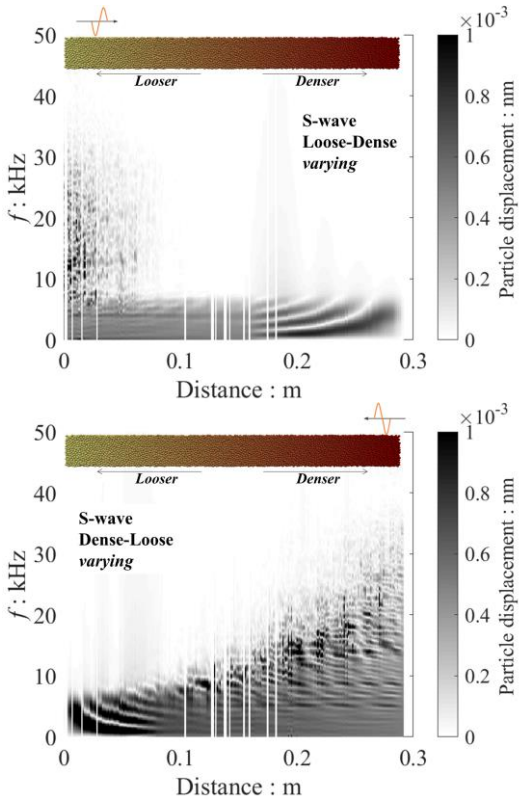

Figure 11. Frequency filtering for S-waves along the varying sample (top) Loose to dense (bottom) Dense to loose.

8. Conclusions

This contribution discussed the influence of locally loosened soil around a subsurface cavity on the wave propagation. Acknowledging that detecting a subsurface cavity is practically difficult, this contribution provides several fundamental dynamic wave responses of granular materials, influenced by density change. Two types of simplified DEM models were adopted to investigate the effects of sharp or gradual change in packing density.

Macroscopic responses of wave velocity (V_P and V_S) and lowpass frequency (f_{lp}) exhibit a qualitatively good agreement between laboratory model tests and DEM simulations. Based on microscopic analyses in DEM models, the following conclusions can be drawn.

- V_P, V_S and f_{lp} decrease in loosened soil, whereas the decrease in f_{lp} is more sensitive.
- V_P or V_S measured during in-situ tests can be an averaged value of V_P or V_S for the wave path measured.
- f_{lp} measured during in-situ tests corresponds to the lowest value of f_{lp} for the wave path measured.
- Wave reflection occurs when the density changes sharply as the acoustic impedance changes sharply.

Further research is needed to link the findings above to in-situ cross-hole or down-hole seismic surveys to improve a better detection method for subsurface cavities.

Acknowledgement

The project presented in this article is supported by JSPS KAKENHI Grant Number 19K15084.

References

[1] Atkinson, J. "Non-linear soil stiffness in routine design", Géotechnique 50(5), pp. 487–508, 2000. https://doi.org/10.1680/geot.2000.50.5.487

[2] Clayton, C. R. I. "Stiffness at small strain: research and practice", Géotechnique 61(1), pp. 5–37, 2011. https://doi.org/10.1680/geot.2011.61.1.5

[3] Kominami, N., 2018. "The relationship between sinkholes and waterpaths and the effectiveness of underground water sound", Master thesis, University of Tokyo, Tokyo, Japan.

[4] Nakata, Y., 2020. "Stress transmission around an underground cavity evaluated using elastic waves", Master thesis, The University of Tokyo.

[5] Ali, U., 2020. "Experimental and numerical analyses of soil arching and stability mechanism under trapdoor and underground cavity conditions", Ph.D. thesis, The University of Tokyo.

[6] Otsubo, M., O'Sullivan, C., Hanley, K. J., Sim, W. "Influence of packing density and stress on the dynamic response of granular materials", Granular Matter, 19(50), pp. 1–18, 2017. https://doi.org/10.1007/s10035-017-0729-2

[7] Plimpton, S. "Fast parallel algorithms for short-range molecular-dynamics", Journal of Computational Physics 117(1), pp. 1–19, 1995. https://doi.org/10.1006/jcph.1995.1039

[8] Itasca Consulting Group "PFC3D version 4.0 user manual", Minneapolis, MN, USA, 2007.

[9] Lawney, B. P., Luding, S. "Frequency filtering in disordered granular chains", Acta Mechanica 225(8), pp. 2385–2407, 2014. https://doi.org/10.1007/s00707-014-1130-4

[10] Mouraille, O., Luding, S. "Soundwave propagation in weakly poly-disperse granular materials", Ultrasonics 48(6-7), pp. 498–505, 2008. https://doi.org/10.1016/j.ultras.2008.03.009

[11] Santamarina, J. C., Klein, K. A., Fam, M. A. "Soils and Waves", Wiley, Hoboken, New Jersey, 2001.

[12] Dutta, T. T., Otsubo, M., Kuwano, R., O'Sullivan, C. "Stress wave velocity in soils: Apparent grain-size effect and optimum input frequencies", Géotechnique Letters, 9(4), pp. 340–347, 2019. https://doi.org/10.1680/jgele.18.00219